

# Reversed Plasma Catalysis Process Design for Efficient Ammonia Decomposition

Frea Van Steenweghen,<sup>§</sup> Annabel Verschueren,<sup>§</sup> Igor Fedirchuk,<sup>§</sup> Johan A. Martens,<sup>\*</sup> Annemie Bogaerts, and Lander Hollevoet



Cite This: *ACS Sustainable Chem. Eng.* 2025, 13, 737–743



Read Online

ACCESS |



Metrics & More



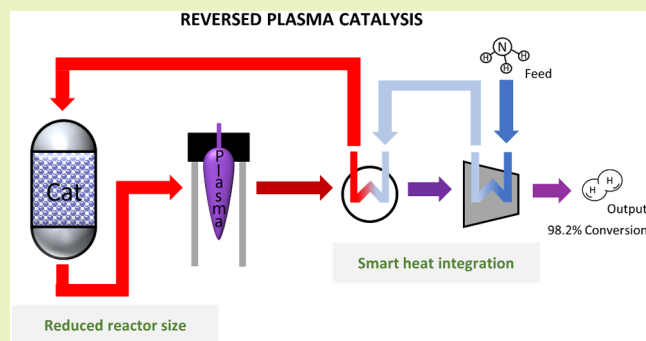
Article Recommendations



Supporting Information

**ABSTRACT:** An innovative process design for ammonia decomposition through *reversed plasma catalysis* is proposed. *Reversed plasma catalysis* involves a partial thermocatalytic conversion of the ammonia feed prior to a warm plasma conversion process of residual ammonia. Lab-scale experiments confirm the potential to achieve 98.2% ammonia conversion using a ruthenium-based catalyst in combination with a Gliding Arc Plasmatron (GAP). Process modeling reveals an efficiency gain of using the excess heat available from the warm plasma reactor to support the endothermic thermocatalytic ammonia cracking. In this study, the *reversed plasma catalysis* process was compared to *thermocatalysis* and *plasma catalysis* process designs under identical reactor conditions, revealing similar energy and exergy efficiency for *plasma catalysis* and *reversed plasma catalysis*. The significant advantage of *reversed plasma catalysis* is the major catalyst savings up to 60% compared to *plasma catalysis* and *thermocatalysis*. These catalyst savings also reduce the reactor size, making *reversed plasma catalysis* a promising approach for efficient ammonia decomposition.

**KEYWORDS:** Ammonia decomposition, plasma catalysis, hydrogen production, warm plasma, heterogeneous catalysis, ruthenium catalyst, exergy analysis, heat integration



## INTRODUCTION

Ammonia ( $\text{NH}_3$ ) has emerged as promising hydrogen carrier due to its high volumetric hydrogen atom content, ease of liquefaction, and existing infrastructure.<sup>1–4</sup> The key remaining challenge is the development of a technology for large-scale ammonia decomposition. Substantial research efforts are being directed toward developing affordable, energy-efficient, and flexible ammonia decomposition processes.<sup>1,4,5</sup>

The most widely explored option is thermocatalytic cracking, but it is limited by the thermodynamic equilibrium of maximum ammonia conversion levels.<sup>6</sup> The  $\text{NH}_3$  decomposition reaction is thermodynamically favored at elevated temperatures ( $>300\text{ }^\circ\text{C}$ ) and low pressures (1 bar).<sup>7</sup> At  $350\text{ }^\circ\text{C}$ , the theoretical maximum conversion is limited to 99%. In theory, gaining additional conversion up to, e.g., 99.9% necessitates heating to  $530\text{ }^\circ\text{C}$ . In practice, achieving such high  $\text{NH}_3$  conversion requires temperatures of  $600\text{--}800\text{ }^\circ\text{C}$ .<sup>8</sup> Heating the gas feed and catalyst bed to such high temperatures requires energy and, therefore, reduces the energy efficiency. Operation at high temperatures also limits the catalyst lifetime. Moreover, elevated temperatures are typically generated by combusting fuel, which may be natural gas or the hydrogen ( $\text{H}_2$ ) product itself, or the  $\text{NH}_3$  feed.<sup>8,9</sup> The first option entails  $\text{CO}_2$  emission, causing the process to

lose its green label, while the second and third options lower the hydrogen yield. One way to reduce the required temperature while maintaining high  $\text{NH}_3$  conversions is to increase the residence time, which can be achieved by enlarging the reactor and increasing the amount of catalyst.<sup>10</sup> However, this significantly impacts the cost.

Plasma technology is a promising alternative to overcome the thermodynamic limitations of endothermic cracking reactions. Plasma is an ionized gas with free electrons, ions, radicals, vibrationally and electronically excited molecules, and photons.<sup>11,12</sup> The energetic electrons activate molecules of the gas which itself does not have to be heated.<sup>12</sup> Additionally, plasma reactors are powered by electricity and can be quickly switched on/off, enabling the utilization of renewable intermittent electricity sources.<sup>11,13</sup>

Plasmas are classified into three main types: cold, which has high-energy electrons but keeps gas molecules unheated;

**Received:** October 25, 2024

**Revised:** January 2, 2025

**Accepted:** January 3, 2025

**Published:** January 8, 2025

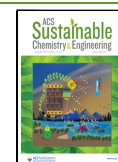


Table 1. Overview of Experimental Atmospheric-Pressure Plasma-Catalytic NH<sub>3</sub> Cracking from the Literature<sup>a</sup>

Plasma	Catalyst	Design	NH <sub>3</sub> feed concentration (%)	T <sub>o</sub> (°C)	NH <sub>3</sub> Conv. (%)	Energy cost (kJ mol <sub>NH<sub>3</sub></sub> <sup>-1</sup> )	ref
DBD	Fe <sub>2</sub> N	In-plasma	100	410	100	841	24
DBD	Co/SiO <sub>2</sub>	In-plasma	100	450	99.2	755	25
DBD	Fe-Ni/SiO <sub>2</sub>	In-plasma	100	500	100	540	26
DBD	Co/SiO <sub>2</sub>	In-plasma	100	380	98	343	27
DBD	Ru/Al <sub>2</sub> O <sub>3</sub>	In-plasma	0.5	RT	86	157,000	28
DBD	MgAl <sub>2</sub> O <sub>4</sub>	In-plasma	100	RT	15.1	2494	29
DBD	Ru/La <sub>2</sub> O <sub>3</sub>	In-plasma	100	380	99.9	404	30
DBD	Ru/La <sub>2</sub> O <sub>3</sub>	In-plasma	100	RT	20	2017	30
DBD	Mo <sub>2</sub> N	In-plasma	100	490	92	1462	31
DBD	Mo <sub>2</sub> N	In-plasma	100	RT	100	888	32
DBD	Ni/Al <sub>2</sub> O <sub>3</sub>	In-plasma	15	435	99.6	3601	18
NTAP	NiO/Al <sub>2</sub> O <sub>3</sub>	Post-plasma	100	RT	20	157	19
GA	Ba-Co/CeO <sub>2</sub>	Post-plasma	50	RT	70	384	33

<sup>a</sup>Energy cost (kJ mol<sub>NH<sub>3</sub></sub><sup>-1</sup>) does not include compression of product gas from 0.1 to 5 MP.

thermal, in which the electrons and gas molecules reach similar high temperature (~10,000 °C); and warm, with similar electron temperatures but with gas temperatures below ~5000 °C.<sup>14</sup> Due to the low gas temperature in cold plasma, nonequilibrium conditions caused by molecular transformations persist best in the reaction products.<sup>12</sup> In the case of ammonia decomposition, state-of-the-art cold plasma processes do not meet the high conversion and low energy consumption requirements.<sup>15</sup> The reason is that the electrons mainly give rise to electronic excitation and ionization, which requires more energy than is strictly needed, and this excess energy is wasted. Vibrational excitation is more important in a warm plasma. In warm plasma, the product composition may reflect the thermodynamic equilibria at very high temperatures, overcoming the thermodynamic equilibrium limitations of the NH<sub>3</sub> decomposition reaction at lower temperatures.<sup>16</sup> Thus, the NH<sub>3</sub> decomposition process in warm plasma is free from the influence of a reverse reaction, which is not thermodynamically favored under these conditions. Nevertheless, warm plasma struggles to reach high NH<sub>3</sub> conversions despite its more favorable energy consumption.<sup>14</sup>

The combined use of plasma and catalyst in so-called *plasma catalysis* has been proposed to improve the performance of chemical conversion processes. Plasma enables additional reaction pathways, which may be unavailable on solid catalysts.<sup>17</sup> Positioning a catalyst inside plasma is possible in cold plasma reactors, such as those with dielectric barrier discharge (DBD), which are the most studied subset of reactors for plasma-catalytic NH<sub>3</sub> cracking (Table 1). For instance, Wang et al. (2024) reached about 100% conversion, but at the expense of a high energy cost of 888 kJ mol<sub>NH<sub>3</sub></sub><sup>-1</sup> using a DBD featuring an in-plasma Mo<sub>2</sub>N catalyst.<sup>18</sup> The research into plasma-catalytic conversion in warm plasmas has been limited to a few works using gliding arc (GA) reactors in post-plasma configuration. In one case, a warm plasma reactor of the nonthermal arc plasma type (NTAP) having a post-plasma NiO/Al<sub>2</sub>O<sub>3</sub> catalyst has been reported achieving a record low energy cost of 157 kJ mol<sub>NH<sub>3</sub></sub><sup>-1</sup>, but the NH<sub>3</sub> conversion was limited to ca. 20%.<sup>19</sup> *Plasma catalysis*, such as DBD with an in-plasma catalyst, can achieve high conversions but has very low energy efficiency.<sup>20,21</sup> Moreover, the physical combination of plasma and catalyst may present challenges for catalyst stability, especially in conditions provided by warm plasma.<sup>22,23</sup>

We propose an alternative process design for ammonia decomposition, namely *reversed plasma catalysis*, having a thermocatalyst positioned in front of the plasma reactor instead of inside or after (Figure 1).<sup>34</sup> A complex sort of

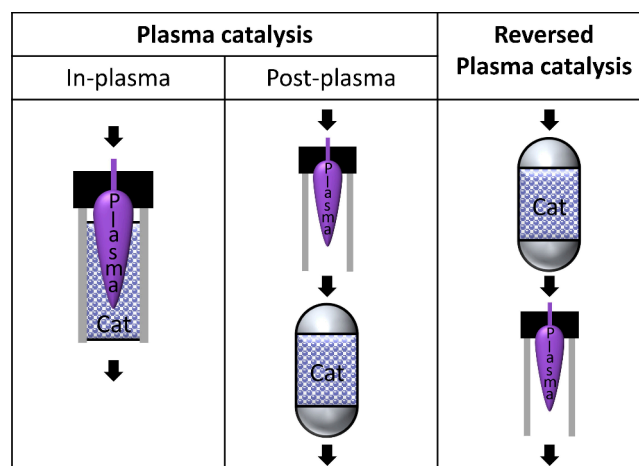


Figure 1. Plasma catalysis (in-plasma and post-plasma) and reversed plasma catalysis process designs.

*reversed plasma catalysis* having a thermocatalyst (Ni/Al<sub>2</sub>O<sub>3</sub>) in front of a plasma membrane reactor achieving decomposition combined with hydrogen separation through a membrane has been proposed in literature.<sup>35</sup> High NH<sub>3</sub> conversion levels of up to 99.9% were reached, but the energy consumption was high, viz. 696 kJ mol<sub>NH<sub>3</sub></sub><sup>-1</sup>.<sup>36</sup> Evidence for clear advantages of reversing the order of the processes has not yet been provided.

The concept of *reversed plasma catalysis* was evaluated through a combination of experiments and computational simulation. *Reversed plasma catalysis* was compared to *thermocatalysis* and *plasma catalysis* regarding energy and exergy use (kJ mol<sub>NH<sub>3</sub></sub><sup>-1</sup>), and catalyst use (g<sub>cat</sub> h mol<sub>NH<sub>3</sub></sub><sup>-1</sup>). The latter parameter also reflects the required thermocatalytic reactor size.

## RESULTS AND DISCUSSION

Partial NH<sub>3</sub> cracking can be conducted efficiently on a thermocatalyst without requiring temperatures exceeding 500 °C, avoiding expensive reactor construction materials.<sup>7,37</sup> Reaching the NH<sub>3</sub> conversion limit dictated by the

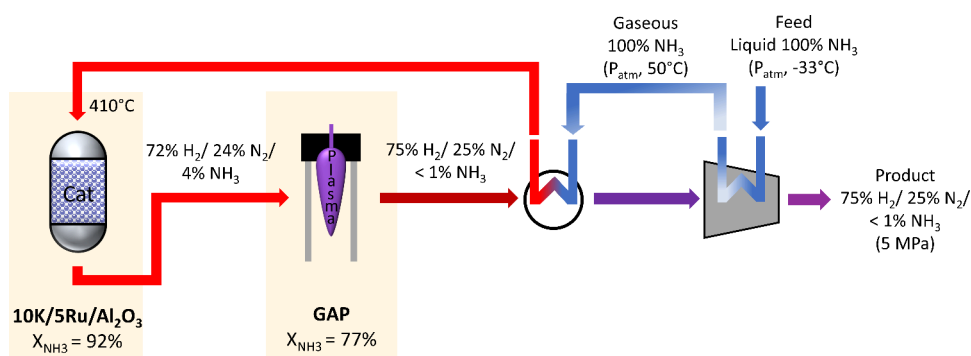


**Figure 2.** Scheme of *reversed plasma catalysis* process, comprising a thermocatalytic reactor with 10K/5Ru/Al<sub>2</sub>O<sub>3</sub> catalyst (1), a GAP plasma reactor (2), a heat exchanger (3), and a compressor (4). Conversions are obtained from experimental data. Heat integration is indicated by heat exchangers between compressor and liquid feed and hot plasma outlet stream and gaseous feed.

thermodynamic equilibrium between ammonia and its decomposition products is very demanding for a thermocatalytic reactor. Conversely, plasma is energy-intensive for converting NH<sub>3</sub>, but it is well-suited for achieving the conversion of residual unconverted NH<sub>3</sub> left over after thermocatalytic decomposition. Plasma operates on electric power, which is partially converted into chemical energy in the endothermic NH<sub>3</sub> cracking reaction and partially converted into heat, especially in thermal and warm plasma.<sup>38</sup> This excess heat can serve as a heat source for the endothermic thermocatalytic process. Moreover, plasma reactors have a simple design, and do not need expensive materials.<sup>39</sup> The power supply constitutes the primary contributor to the capital cost of the plasma reactor, which is expected to decrease with technological advancements and large-scale adoption of plasma technology, ultimately resulting in a lower overall CAPEX.

A particularly effective catalyst described in the literature was selected, viz. potassium-promoted ruthenium on alumina.<sup>7,40</sup> The catalyst, denoted as 10K/5Ru/Al<sub>2</sub>O<sub>3</sub>, was synthesized using incipient wetness impregnation of subsequent Ru and K precursors onto alumina with nominal weight ratios of 10/5/100. The catalytic performance was evaluated in a continuous flow fixed bed microreactor using a pure NH<sub>3</sub> flow. Experimental details can be found in the [Supporting Information](#) (SI, section 1).

The most efficient warm plasma reactor type was found to be the Gliding Arc Plasmatron (GAP),<sup>14</sup> which was also proven effective for other gas conversion applications.<sup>41–43</sup> This plasma reactor was fed with a gas mixture simulating the outlet of the thermocatalytic reactor. Experimental details can be found in SI (section 2).

The thermocatalytic reactor reached an NH<sub>3</sub> conversion of 92.3% at 410 °C at a WHSV of 4.4 h<sup>-1</sup> (GHSV of 5800 mL<sub>NH<sub>3</sub></sub> g<sub>cat</sub><sup>-1</sup> h<sup>-1</sup>). The reaction product has a gas composition of 4 vol % NH<sub>3</sub>, 72 vol % H<sub>2</sub>, and 24 vol % N<sub>2</sub>. Using such mixture as feed, the GAP plasma reactor decomposed 77.2% of the NH<sub>3</sub> contained in this gas mixture at a reaction rate of 0.06 mol<sub>NH<sub>3</sub></sub>·h<sup>-1</sup> with an energy consumption of 1,600 kJ per mol of cracked NH<sub>3</sub> by plasma. Based on literature data,<sup>44–46</sup> specifications of existing commercial plasma devices (e.g., Hypertherm HPR400XD, Oerlikon-Metco FlexiArc 300), and experimental results obtained with suboptimally matched power supplies,<sup>14</sup> it can be reasonably assumed that, with proper matching to the plasma setup, the power supply efficiency can reach at least 90%. Using this efficiency value as a baseline, the actual energy consumption amounts to 1750 kJ

per mol of cracked NH<sub>3</sub> by plasma. This energy requirement pertains to the two reactors in the *reversed plasma catalysis* process as the plasma reactor delivers the heat for the thermocatalytic reactor. Consequently, the overall energy cost of cracking the ammonia feed is 105 kJ/mol of NH<sub>3</sub> converted through *reversed plasma catalysis*.

**Figure 2** represents the process scheme of the *reversed plasma catalysis* process with a thermocatalytic reactor (1) followed by a GAP plasma reactor (2). A heat exchanger (3) is added to recover the heat generated in the plasma reactor and use it to heat the thermocatalytic reactor. A compressor (4) is added to compress the produced gas to 5 MPa.

The *reversed plasma catalysis* process was simulated by using the Aspen Plus V14 software. The input data can be found in SI (section 3, Table S1). The feed is liquid pure NH<sub>3</sub> at -33 °C and atmospheric pressure.<sup>1</sup> The cold NH<sub>3</sub> feed is evaporated and heated to 410 °C via heat exchangers with heat coming from the compressor and the hot product gas. Well-insulated heat exchangers were assumed with a significant temperature difference between the hot inlet and the cold outlet. The hot feed is directed into the thermocatalytic reactor, decomposing 92.3% of the pure NH<sub>3</sub> feed. The outlet gas mixture contains 4 vol % NH<sub>3</sub> and is fed into the GAP plasma reactor, which converts 77.2% of this remaining NH<sub>3</sub>. The plasma reactor is simulated as a combination of a heater and a reactor making no byproducts. The hot product gas of the plasma reactor has an outlet temperature of about 2000 °C, which agrees well with literature-based experiments with the same plasma reactor.<sup>47</sup> The hot gas serves as a heat source for maintaining the catalytic reactor at its operating temperature of 410 °C and preheating the NH<sub>3</sub> feed. The overall NH<sub>3</sub> conversion reaches 98.2%, of which 92.3% is achieved by thermocatalysis and 5.9% is achieved by warm plasma. The final gas composition at the outlet of the *reversed plasma catalysis* process corresponds to 0.9 vol % NH<sub>3</sub>, 74.3 vol % H<sub>2</sub>, and 24.8 vol % N<sub>2</sub>. The remaining 0.9 vol % NH<sub>3</sub> in the gas product could be purified downstream using separation techniques, such as adsorption.<sup>7,48,49</sup> However, approaching full conversion in a single pass process is crucial to avoid significant energy penalties and increased complexity associated with the additional separation steps and the recirculation of large quantities of ammonia. A 4-stage compressor located downstream compresses the product gas to 5 MPa, the desired gas pressure in hydrogen pipelines.<sup>50</sup> Four stages are needed due to the maximal allowable discharge temperature of around 150 °C in reciprocating compressors.<sup>51</sup> The additional heat

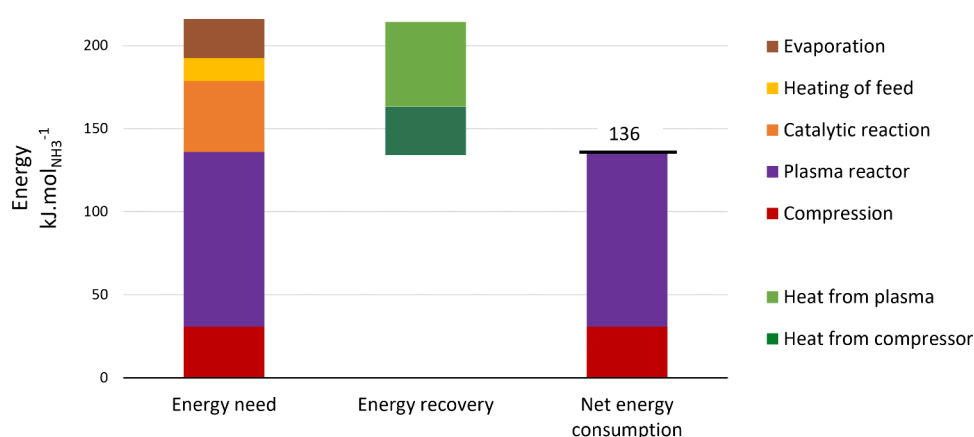


**Figure 3.** Energy requirements of the *reversed plasma catalysis* process with energy recovery.

created by the compressor is used to evaporate the liquid  $\text{NH}_3$  feed.

The energy consumed by the different unit operations: evaporation and heating of the feed, the heat requirement for the endothermic cracking reaction in the catalytic reactor, and work for operating the plasma reactor as well as the compressor, are presented in **Figure 3**. The excess heat generated by plasma and compressor can be recovered as heat required for  $\text{NH}_3$  evaporation, preheating, and catalytic cracking. Therefore, the net energy consumption ( $136 \text{ kJ mol}_{\text{NH}_3}^{-1}$ ) is entirely determined by the plasma process ( $105 \text{ kJ mol}_{\text{NH}_3}^{-1}$ ) and compression ( $31 \text{ kJ mol}_{\text{NH}_3}^{-1}$ ).

To demonstrate the potential of the *reversed plasma catalysis* process, it was experimentally compared to both the *thermocatalysis* and *plasma catalysis* (post-plasma) process designs. The processes were operated under identical conditions: at the same current and gas flow rate for the GAP plasma reactor and at the same temperature for the catalytic reactor. In all cases, the  $\text{NH}_3$  conversion reached 98.2%. The plasma process alone was disregarded, as it was not able to reach the 98.2% conversion target as standalone technology. More specifically, the GAP plasma reactor, operating under the same conditions, reaches only 24% conversion of pure  $\text{NH}_3$  with an energy consumption of 231 kJ per mol  $\text{NH}_3$  converted in the plasma reactor.

The thermocatalytic process achieves the target 98.2%  $\text{NH}_3$  conversion at  $410^\circ\text{C}$  at a WHSV of  $1.6 \text{ h}^{-1}$ , corresponding to a catalyst contact time of  $10.6 \text{ g}_{\text{cat}} \text{ h mol}_{\text{NH}_3}^{-1}$ . In this process design, no smart heat integration is possible, necessitating external heating for both the feed and catalytic reactor. In the *plasma catalysis* process, the GAP reactor decomposes 38% of the  $\text{NH}_3$  feed with an energy consumption of 644 W. In order to obtain the 98.2% overall conversion, the catalyst has to decompose 97.1% of the remaining  $\text{NH}_3$ , which, at  $410^\circ\text{C}$ , could be reached at a WHSV of  $1.9 \text{ h}^{-1}$ , corresponding to a catalyst contact time of  $8.8 \text{ g}_{\text{cat}} \text{ h mol}_{\text{NH}_3}^{-1}$ .

The experimental results were further analyzed through process simulations in Aspen Plus to determine the net energy consumption, incorporating smart heat integration between the plasma and catalytic reactors as well as between the compressor and feed. The process schemes made by Aspen for the three process designs can be found in **SI** (section 3). However, a more significant parameter for evaluating these processes is the net exergy consumption, which accounts for the useful excess heat generated.<sup>52</sup> Net exergy consumption is

determined by subtracting the useful exergy output from the total exergy input. The total exergy input is the electricity powering the plasma reactor and compressor, along with the chemical exergy of the  $\text{NH}_3$  feed. The useful exergy output consists of the chemical exergy of the product and the exergy of the excess heat, which increases with its temperature.<sup>53,54</sup> Detailed calculations are provided in **SI** (section 4). The net energy consumption, net exergy consumption, and catalyst need for the three processes are summarized in **Table 2**.

**Table 2.** Comparison of Process Performance Characteristics to Obtain a 98.2% Overall  $\text{NH}_3$  Conversion with 100% Liquid  $\text{NH}_3$  Feed and 5 MPa Product Pressure for *Thermocatalysis* (10K/5Ru/ $\text{Al}_2\text{O}_3$ ,  $410^\circ\text{C}$ ), *Plasma Catalysis* (GAP,  $10 \text{ nL min}^{-1}$   $\text{NH}_3$  flow rate, 644 W – 10K/5Ru/ $\text{Al}_2\text{O}_3$ ,  $410^\circ\text{C}$ ), and *Reversed Plasma Catalysis* (10K/5Ru/ $\text{Al}_2\text{O}_3$ ,  $410^\circ\text{C}$  – GAP,  $20 \text{ nL min}^{-1}$  total flow rate with 4 vol%  $\text{NH}_3$ , 723W)

Process design	<i>Thermocatalysis</i>	<i>Plasma catalysis</i> (post-plasma)	<i>Reversed plasma catalysis</i>
Net energy consumption ( $\text{kJ mol}_{\text{NH}_3}^{-1}$ )	78.2	128	136
Net exergy consumption ( $\text{kJ mol}_{\text{NH}_3}^{-1}$ )	46.3	60.4	60.5
Catalyst need ( $\text{g}_{\text{cat}} \text{ h mol}_{\text{NH}_3}^{-1}$ )	10.6	8.8	3.9

In terms of net energy consumption, the *thermocatalysis* process remains the most efficient. *Plasma catalysis* shows a slightly lower energy consumption than the reversed process, due to the higher efficiency of the plasma reactor when operating with a pure  $\text{NH}_3$  feed. In addition, both *plasma catalysis* and *reversed plasma catalysis* processes from this study outperform plasma-based processes reported in the literature (**Table 1**), which predominantly use cold plasma. The superior performance can be attributed to the benefits of using a warm plasma, i.e., its higher energy efficiency, and effective utilization of excess heat as a source for catalytic cracking. Moreover, none of the processes reported in literature account for the energy cost of compressing the hydrogen product. The similar net exergy consumption for the *plasma catalysis* and *reversed plasma catalysis* concepts reflects the high-quality heat generated in the *reversed plasma catalysis* process. To further optimize energy and exergy consumption, plasma energy

consumption should ideally approach the theoretical minimum of 55 kJ mol<sub>NH<sub>3</sub></sub><sup>-1</sup>.

The most salient feature of *reversed plasma catalysis* is its drastically lower catalyst requirement, which is two times lower than that in *plasma catalysis* and almost three times lower than that in *thermocatalysis*. Positioning the catalyst upstream of the plasma reactor not only reduces the catalyst cost but also the size of the thermocatalytic reactor, significantly lowering installation costs. While *thermocatalysis* exhibits lower energy consumption, the *reversed plasma catalysis* process stands out due to its significantly reduced catalyst demand, enabling a much smaller catalytic reactor size. Future improvements in energy efficiency of the plasma reactor can reduce the amount of excess heat generated and therefore lower the energy cost while maintaining the same advantage in smaller reactor size.

## CONCLUSIONS

This study highlights the potential of *reversed plasma catalysis* as an alternative ammonia decomposition process design. The innovative *reversed plasma catalysis* process allows the use of the excess heat created by warm plasma in the catalytic process, resulting in high conversions at a moderate catalyst temperature (410 °C). An overall conversion of 98.2% was achieved, with 92% accomplished through ruthenium-based thermocatalysis and 6% through warm plasma. As a future perspective, replacing ruthenium with a nonprecious metal is a viable strategy because of the low temperature (410 °C) and the moderate conversion rate requirement (92%) in the thermocatalytic reactor (Figure 2).

A comparative study of plasma catalysis and *reversed plasma catalysis* revealed similar net energy and exergy consumption, which are both substantially lower than those previously reported in the literature (Table 1). However, compared to *thermocatalysis*, the *reversed plasma catalysis* process is not yet as energy efficient. Improving the energy efficiency of the plasma reactor is crucial for enhancing the overall energy performance. Notably, the *reversed plasma catalysis* process requires only half of the catalyst mass needed in *plasma catalysis* and almost one-third of that in *thermocatalysis* (Table 2). This results in substantial catalyst savings and the downsizing of the reactor. This advantage positions the *reversed plasma catalysis* process as a competitive alternative for ammonia decomposition.

## ASSOCIATED CONTENT

### Supporting Information

The Supporting Information is available free of charge at <https://pubs.acs.org/doi/10.1021/acssuschemeng.4c08899>.

Sections 1 and 2: Detailed experimental procedures for thermocatalytic cracking and plasma cracking, including lab setup, operating conditions, and catalyst description. Section 3: Aspen Plus input data used for process modeling and simulation of the *reversed plasma catalysis* process, including component specifications and process parameters. Aspen Plus process schemes for the three compared processes. Section 4: Exergy analysis of the three compared processes, including equations and results. (PDF)

## AUTHOR INFORMATION

### Corresponding Author

Johan A. Martens – Surface Chemistry and Catalysis: Characterization and Application Team (COK-KAT), KU Leuven, Leuven, BE 3001, Belgium; [orcid.org/0000-0002-9292-2357](https://orcid.org/0000-0002-9292-2357); Email: [johan.martens@kuleuven.be](mailto:johan.martens@kuleuven.be)

### Authors

Frea Van Steenweghen – Surface Chemistry and Catalysis: Characterization and Application Team (COK-KAT), KU Leuven, Leuven, BE 3001, Belgium; [orcid.org/0000-0002-1687-7136](https://orcid.org/0000-0002-1687-7136)

Annabel Verschuere – Surface Chemistry and Catalysis: Characterization and Application Team (COK-KAT), KU Leuven, Leuven, BE 3001, Belgium; [orcid.org/0009-0008-3404-7022](https://orcid.org/0009-0008-3404-7022)

Igor Fedirchuk – Research group PLASMANT, Department of Chemistry, University of Antwerp, Wilrijk, BE 2610, Belgium

Annemie Bogaerts – Research group PLASMANT, Department of Chemistry, University of Antwerp, Wilrijk, BE 2610, Belgium; [orcid.org/0000-0001-9875-6460](https://orcid.org/0000-0001-9875-6460)

Lander Hollevoet – Surface Chemistry and Catalysis: Characterization and Application Team (COK-KAT), KU Leuven, Leuven, BE 3001, Belgium; [orcid.org/0000-0003-0052-080X](https://orcid.org/0000-0003-0052-080X)

Complete contact information is available at:

<https://pubs.acs.org/10.1021/acssuschemeng.4c08899>

### Author Contributions

<sup>§</sup>F.V.S., A.V., and I.F. contributed equally. F.V.S.: investigation, data curation, visualization, funding acquisition, writing—original draft. A.V.: investigation, data curation. I.F.: investigation, data curation, funding acquisition, writing—original draft. J.A.M.: supervision, project administration, funding acquisition, writing—review and editing. A.B.: supervision, project administration, funding acquisition, writing—review and editing. L.H.: formal analysis, conceptualization, validation, funding acquisition, writing—review and editing. All authors have given approval to the final version of the manuscript.

### Notes

The authors declare no competing financial interest.

## ACKNOWLEDGMENTS

This work was supported by the HyPACT project funded by the Belgian Energy Transition Fund. J.A.M. and A.B. gratefully acknowledge the Flemish Government for long-term structural funding (Methusalem). J.A.M. acknowledges KU Leuven for an internal grant from the Industrial Research Fund (project No. C3/20/067). F.V.S. acknowledges Research Foundation Flanders (FWO) for an FWO-SB fellowship (No. 1S58723N). L.H. also acknowledges Flanders Innovation & Entrepreneurship for an innovation mandate (No. HBC.2023.0674). I.F. acknowledges the MSCA4Ukraine project 1233629 funded by the European Union.

## ABBREVIATIONS

NH<sub>3</sub>, ammonia; H<sub>2</sub>, hydrogen; N<sub>2</sub>, nitrogen

## REFERENCES

- (1) *Innovation Outlook: Renewable Ammonia*; International Renewable Energy Agency (IRENA); Ammonia Energy Association (AEA): Abu Dhabi, Brooklyn, 2022; Vol. 144.
- (2) Hasan, M. H.; Mahlia, T. M. I.; Mofijur, M.; Rizwanul Fattah, I. M.; Handayani, F.; Ong, H. C.; Silitonga, A. S. A Comprehensive Review on the Recent Development of Ammonia as a Renewable Energy Carrier. *Energies (Basel)* **2021**, *14* (13), 3732.
- (3) Cha, J.; Jo, Y. S.; Jeong, H.; Han, J.; Nam, S. W.; Song, K. H.; Yoon, C. W. Ammonia as an Efficient CO<sub>x</sub>-Free Hydrogen Carrier: Fundamentals and Feasibility Analyses for Fuel Cell Applications. *Appl. Energy* **2018**, *224*, 194–204.
- (4) Spatolisano, E.; Pellegrini, L. A.; De Angelis, A. R.; Cattaneo, S.; Roccaro, E. Ammonia as a Carbon-Free Energy Carrier: NH<sub>3</sub> Cracking to H<sub>2</sub>. *Ind. Eng. Chem. Res.* **2023**, *62* (28), 10813–10827.
- (5) Weichenhain, U. Hydrogen Transportation, 2021. Roland Berger GmbH. <https://www.rolandberger.com/en/Insights/Publications/Transporting-the-fuel-of-the-future.html> (accessed 2024–05–22).
- (6) Li, N.; Zhang, C.; Li, D.; Jiang, W.; Zhou, F. Review of Reactor Systems for Hydrogen Production via Ammonia Decomposition. *Chemical Engineering Journal* **2024**, *495*, No. 153125.
- (7) Lucentini, I.; Garcia, X.; Vendrell, X.; Llorca, J. Review of the Decomposition of Ammonia to Generate Hydrogen. *Ind. Eng. Chem. Res.* **2021**, *60* (51), 18560–18611.
- (8) Yousefi Rizi, H.; Shin, D. Green Hydrogen Production Technologies from Ammonia Cracking. *Energies (Basel)* **2022**, *15* (21), 8246.
- (9) Kang, Z.; Liu, B.; Huang, J.; Fan, H.; Wang, K. A Hydrogen Production System Based on Ammonia Combustion Heat: Graded Decomposition and Parameter Analysis. *E3S Web of Conferences* **2024**, *520*, 03010.
- (10) Chein, R. Y.; Chen, Y. C.; Chang, C. S.; Chung, J. N. Numerical Modeling of Hydrogen Production from Ammonia Decomposition for Fuel Cell Applications. *Int. J. Hydrogen Energy* **2010**, *35* (2), 589–597.
- (11) Bogaerts, A.; Centi, G.; Hessel, V.; Rebrov, E. Challenges in Unconventional Catalysis. *Catal. Today* **2023**, *420*, No. 114180.
- (12) Bogaerts, A.; Neyts, E. C. Plasma Technology: An Emerging Technology for Energy Storage. *ACS Energy Lett.* **2018**, *3* (4), 1013–1027.
- (13) Bogaerts, A.; Centi, G. Plasma Technology for CO<sub>2</sub> Conversion: A Personal Perspective on Prospects and Gaps. *Front Energy Res.* **2020**, *8* (111), na DOI: 10.3389/fenrg.2020.00111.
- (14) Fedirchuk, I.; Tsonev, I.; Quiroz Marnef, R.; Bogaerts, A. Plasma-Assisted NH<sub>3</sub> Cracking in Warm Plasma Reactors for Green H<sub>2</sub> Production. *Chemical Engineering Journal* **2024**, *499*, No. 155946.
- (15) Gorbanev, Y.; Fedirchuk, I.; Bogaerts, A. Plasma Catalysis in Ammonia Production and Decomposition: Use It, or Lose It? *Curr. Opin Green Sustain Chem.* **2024**, *47*, No. 100916.
- (16) Gutsol, A.; Rabinovich, A.; Fridman, A. Combustion-Assisted Plasma in Fuel Conversion. *J. Phys. D Appl. Phys.* **2011**, *44* (27), No. 274001.
- (17) Bogaerts, A.; Tu, X.; Whitehead, J. C.; Centi, G.; Lefferts, L.; Guaitella, O.; Azzolina-Jury, F.; Kim, H.-H.; Murphy, A. B.; Schneider, W. F.; Nozaki, T.; Hicks, J. C.; Rousseau, A.; Thevenet, F.; Khacef, A.; Carreon, M. The 2020 Plasma Catalysis Roadmap. *J. Phys. D Appl. Phys.* **2020**, *53* (44), No. 443001.
- (18) Zhou, W.; Zhang, W.; Shan, Y.; Liu, B.; Li, K.; Ren, J.; Li, Y.; Zhang, X.; Wang, Z. Carbon-Free Hydrogen Production via Plasma-Catalytic Ammonia Decomposition over Transition Metal-Based Catalysts: In Situ Probing by DRIFTS and SVUV-PIMS. *Chemical Engineering Journal* **2024**, *492*, No. 152101.
- (19) Lin, Q. F.; Jiang, Y. M.; Liu, C. Z.; Chen, L. W.; Zhang, W. J.; Ding, J.; Li, J. G. Instantaneous Hydrogen Production from Ammonia by Non-Thermal Arc Plasma Combining with Catalyst. *Energy Reports* **2021**, *7*, 4064–4070.
- (20) Meng, S.; Li, S.; Sun, S.; Bogaerts, A.; Liu, Y.; Yi, Y. NH<sub>3</sub> Decomposition for H<sub>2</sub> Production by Thermal and Plasma Catalysis Using Bimetallic Catalysts. *Chem. Eng. Sci.* **2024**, *283*, No. 119449.
- (21) Yi, Y.; Wang, L.; Guo, H. Plasma-Catalytic Decomposition of Ammonia for Hydrogen Energy. In *Plasma Catalysis: Fundamentals and Applications*; Tu, X., Whitehead, J. C., Nozaki, T., Eds.; Springer International Publishing: Cham, 2019; pp 181–230.
- (22) Zhang, S.; Oehrlein, G. S. From Thermal Catalysis to Plasma Catalysis: A Review of Surface Processes and Their Characterizations. *J. Phys. D Appl. Phys.* **2021**, *54* (21), No. 213001.
- (23) Loenders, B.; Michiels, R.; Bogaerts, A. Is a Catalyst Always Beneficial in Plasma Catalysis? Insights from the Many Physical and Chemical Interactions. *Journal of Energy Chemistry* **2023**, *85*, 501–533.
- (24) Wang, L.; Zhao, Y.; Liu, C.; Gong, W.; Guo, H. Plasma Driven Ammonia Decomposition on a Fe-Catalyst: Eliminating Surface Nitrogen Poisoning. *Chem. Commun.* **2013**, *49* (36), 3787.
- (25) Wang, L.; Yi, Y.; Zhao, Y.; Zhang, R.; Zhang, J.; Guo, H. NH<sub>3</sub> Decomposition for H<sub>2</sub> Generation: Effects of Cheap Metals and Supports on Plasma-Catalyst Synergy. *ACS Catal.* **2015**, *5* (7), 4167–4174.
- (26) Yi, Y.; Wang, L.; Guo, Y.; Sun, S.; Guo, H. Plasma-assisted Ammonia Decomposition over Fe-Ni Alloy Catalysts for CO<sub>x</sub>-Free Hydrogen. *AIChE J.* **2019**, *65* (2), 691–701.
- (27) Wang, L.; Yi, Y.; Guo, H.; Du, X.; Zhu, B.; Zhu, Y. Highly Dispersed Co Nanoparticles Prepared by an Improved Method for Plasma-Driven NH<sub>3</sub> Decomposition to Produce H<sub>2</sub>. *Catalysts* **2019**, *9* (2), 107.
- (28) El-Shafie, M.; Kambara, S.; Hayakawa, Y. Plasma-Enhanced Catalytic Ammonia Decomposition over Ruthenium (Ru/Al<sub>2</sub>O<sub>3</sub>) and Soda Glass (SiO<sub>2</sub>) Materials. *Journal of the Energy Institute* **2021**, *99*, 145–153.
- (29) Andersen, J. A.; Christensen, J. M.; Østberg, M.; Bogaerts, A.; Jensen, A. D. Plasma-Catalytic Ammonia Decomposition Using a Packed-Bed Dielectric Barrier Discharge Reactor. *Int. J. Hydrogen Energy* **2022**, *47* (75), 32081–32091.
- (30) Wang, Z.; He, G.; Zhang, H.; Liao, C.; Yang, C.; Zhao, F.; Lei, G.; Zheng, G.; Mao, X.; Zhang, K. Plasma-Promoted Ammonia Decomposition over Supported Ruthenium Catalysts for CO<sub>x</sub>-Free H<sub>2</sub> Production. *ChemSusChem* **2023**, *16* (24), No. e202202370.
- (31) Yu, X.; Hu, K.; Zhang, H.; He, G.; Xia, Y.; Deng, M.; Shi, Y.; Yang, C.; Mao, X.; Wang, Z. Plasma-Catalytic Ammonia Decomposition for Carbon-Free Hydrogen Production Using Low Pressure-Synthesized Mo<sub>2</sub>N Catalyst. *Plasma Chemistry and Plasma Processing* **2023**, *43* (1), 183–197.
- (32) Wang, Z.; Zhang, H.; Ye, Z.; He, G.; Liao, C.; Deng, J.; Lei, G.; Zheng, G.; Zhang, K.; Gou, F.; Mao, X. H<sub>2</sub> Production from Ammonia Decomposition with Mo<sub>2</sub>N Catalyst Driven by Dielectric Barrier Discharge Plasma. *Int. J. Hydrogen Energy* **2024**, *49*, 1375–1385.
- (33) Ronduda, H.; Mlotek, M.; Góral, W.; Zybert, M.; Ostrowski, A.; Sobczak, K.; Krawczyk, K.; Raróg-Pilecka, W. Cobalt Catalysts for CO-Free Hydrogen Production: Effect of Catalyst Type on Ammonia Decomposition in Gliding Discharge Plasma Reactor. *Journal of CO<sub>2</sub> Utilization* **2024**, *82*, No. 102755.
- (34) Drake, G. W. F.; Babb, J.; Bandrauk, A. D.; Joachain, C. J. *Plasma Catalysis: Fundamentals and Applications*, 1st ed.; Tu, X., Nozaki, T., Whitehead, J. C., Eds.; Cham, Springer, 2019; Vol. 106.
- (35) Hayakawa, Y.; Miura, T.; Shizuya, K.; Wakazono, S.; Tokunaga, K.; Kambara, S. Hydrogen Production System Combined with a Catalytic Reactor and a Plasma Membrane Reactor from Ammonia. *Int. J. Hydrogen Energy* **2019**, *44* (20), 9987–9993.
- (36) El-Shafie, M.; Kambara, S.; Hayakawa, Y. Energy and Exergy Analysis of Hydrogen Production from Ammonia Decomposition Systems Using Non-Thermal Plasma. *Int. J. Hydrogen Energy* **2021**, *46* (57), 29361–29375.
- (37) Davies, M.; Corrosion Consultants Corrosion by Ammonia. In *Corrosion: Environments and Industries*; ASM International, 2006; pp 727–735. DOI: 10.31399/asm.hb.v13c.a0004185.
- (38) Boulou, M. I. Thermal Plasma Processing. *IEEE Transactions on Plasma Science* **1991**, *19* (6), 1078–1089.

- (39) Snoeckx, R.; Bogaerts, A. Plasma Technology – a Novel Solution for CO<sub>2</sub> Conversion? *Chem. Soc. Rev.* **2017**, *46* (19), 5805–5863.
- (40) Ju, X.; Liu, L.; Zhang, T.; He, T.; Xu, Y.; Chen, P. Ru Nanoparticles on K Doped  $\gamma$ -Alumina with Abundant Surface Superbasic Sites for Ammonia Decomposition. *Catal. Lett.* **2024**, *154* (2), 473–486.
- (41) Nunnally, T.; Gutsol, K.; Rabinovich, A.; Fridman, A.; Gutsol, A.; Kemoun, A. Dissociation of CO<sub>2</sub> in a Low Current Gliding Arc Plasmatron. *J. Phys. D Appl. Phys.* **2011**, *44* (27), No. 274009.
- (42) Vervloessem, E.; Aghaei, M.; Jardali, F.; Hafezkhiani, N.; Bogaerts, A. Plasma-Based N<sub>2</sub> Fixation into NO<sub>x</sub>: Insights from Modeling toward Optimum Yields and Energy Costs in a Gliding Arc Plasmatron. *ACS Sustain Chem. Eng.* **2020**, *8* (26), 9711–9720.
- (43) Slaets, J.; Aghaei, M.; Ceulemans, S.; Van Alphen, S.; Bogaerts, A. CO<sub>2</sub> and CH<sub>4</sub> Conversion in “Real” Gas Mixtures in a Gliding Arc Plasmatron: How Do N<sub>2</sub> and O<sub>2</sub> Affect the Performance? *Green Chem.* **2020**, *22* (4), 1366–1377.
- (44) Stryczewska, H. D. Supply Systems of Non-Thermal Plasma Reactors. Construction Review with Examples of Applications. *Applied Sciences* **2020**, *10* (9), 3242.
- (45) Boulos, M. I.; Fauchais, P. L.; Pfender, E. *Handbook of Thermal Plasmas*; Springer International Publishing, 2023.
- (46) Zhukov, M. F.; Zasyplin, I. M. *Thermal Plasma Torches: Design, Characteristics, Application*; Cambridge International Science Publishing: Cambridge, 2007; Vol. 596.
- (47) Girard-Sahun, F.; Biondo, O.; Trenchev, G.; van Rooij, G.; Bogaerts, A. Carbon Bed Post-Plasma to Enhance the CO<sub>2</sub> Conversion and Remove O<sub>2</sub> from the Product Stream. *Chemical Engineering Journal* **2022**, *442*, No. 136268.
- (48) Abello, M. C.; Velasco, A. P.; Gomez, M. F.; Rivarola, J. B. Temperature-Programmed Desorption of NH<sub>3</sub> on Na-Y Zeolite. *Langmuir* **1997**, *13* (10), 2596–2599.
- (49) Liu, C. Y.; Aika, K. Ammonia Adsorption on Ion Exchanged Y-Zeolites as Ammonia Storage Material. *Journal of the Japan Petroleum Institute* **2003**, *46* (5), 301–307.
- (50) Gillette, J. L.; Kolpa, R. L. Overview of Interstate Hydrogen Pipeline Systems, 2007. Argonne National Laboratory, Environmental Science Division. [https://corridoreis.anl.gov/documents/docs/technical/apt\\_61012\\_evs\\_tm\\_08\\_2.pdf](https://corridoreis.anl.gov/documents/docs/technical/apt_61012_evs_tm_08_2.pdf) (accessed 2024–06–05).
- (51) Application Manual - Heavy Duty Balanced Opposed Reciprocating Compressors, 2023. Ariel Corporation. [www.arielcorp.com](http://www.arielcorp.com).
- (52) El-Shafie, M.; Kambara, S.; Hayakawa, Y. Energy and Exergy Analysis of Hydrogen Production from Ammonia Decomposition Systems Using Non-Thermal Plasma. *Int. J. Hydrogen Energy* **2021**, *46* (57), 29361–29375.
- (53) Wang, L.-S. *A Treatise of Heat and Energy*; Mechanical Engineering Series; Kulacki, F., Ed.; Springer International Publishing: Cham, 2020; Vol. 301. DOI: 10.1007/978-3-030-05746-6.
- (54) Mendonça Teixeira, A.; de Oliveira Arinelli, L.; de Medeiros, J. L.; de Queiroz Fernandes Araújo, O. Exergy Analysis of Chemical Processes. In *SpringerBriefs in Petroleum Geoscience and Engineering*; Springer Nature, 2018; pp 75–82. DOI: 10.1007/978-3-319-66074-5\_8.